Multistep mechanism of substrate binding determines chaperone activity of Hsp70

Matthias P. Mayer[1], Hartwig Schröder[1,2], Stefan Rüdiger[1], Klaus Paal[1], Thomas Laufen[1] and Bernd Bukau[1]

The 70 kDa heat shock proteins (the Hsp70 family) assist refolding of their substrates through ATP-controlled binding. We have analyzed mutants of DnaK, an Hsp70 homolog, altered in key residues of its substrate binding domain. Substrate binding occurs by a dynamic mechanism involving: a hydrophobic pocket for a single residue that is crucial for affinity, a two-layered closing device involving independent action of an α-helical lid and an arch, and a superimposed allosteric mechanism of ATP-controlled opening of the substrate binding cavity that operates largely through a β-structured subdomain. Correlative evidence from mutational analysis suggests that the ADP and ATP states of DnaK differ in the frequency of the conformational changes in the α-helical lid and β-domain that cause opening of the substrate binding cavity. The affinity for substrates, as defined by this mechanism, determines the efficiency of DnaJ-mediated and ATP hydrolysis mediated locking-in of substrates and chaperone activity of DnaK.

The chaperone activity of 70 kDa heat shock proteins (the Hsp70 family) to assist in protein folding relies on their ability to repeatedly associate with short stretches of polypeptides in extended conformations. This reaction is controlled by ATP — binding of ATP to the N-terminal ATPase domain of Hsp70 proteins induces conformational changes in the adjacent substrate binding domain that open the substrate binding cavity (SBC) and result in high association (k_{on}) and dissociation (k_{off}) rate constants for substrates[1,2]. ATP hydrolysis causes the SBC to close and results in low k_{on} and k_{off} for bound substrates. The cochaperone DnaJ[3], in synergy with the bound protein substrate in the SBC, triggers the cleavage of γ-phosphate[4–6], the rate limiting step of the ATPase cycle.

The structure of the substrate binding domain of *Escherichia coli* DnaK, an Hsp70 homolog, in complex with a heptapeptide substrate had been deter-

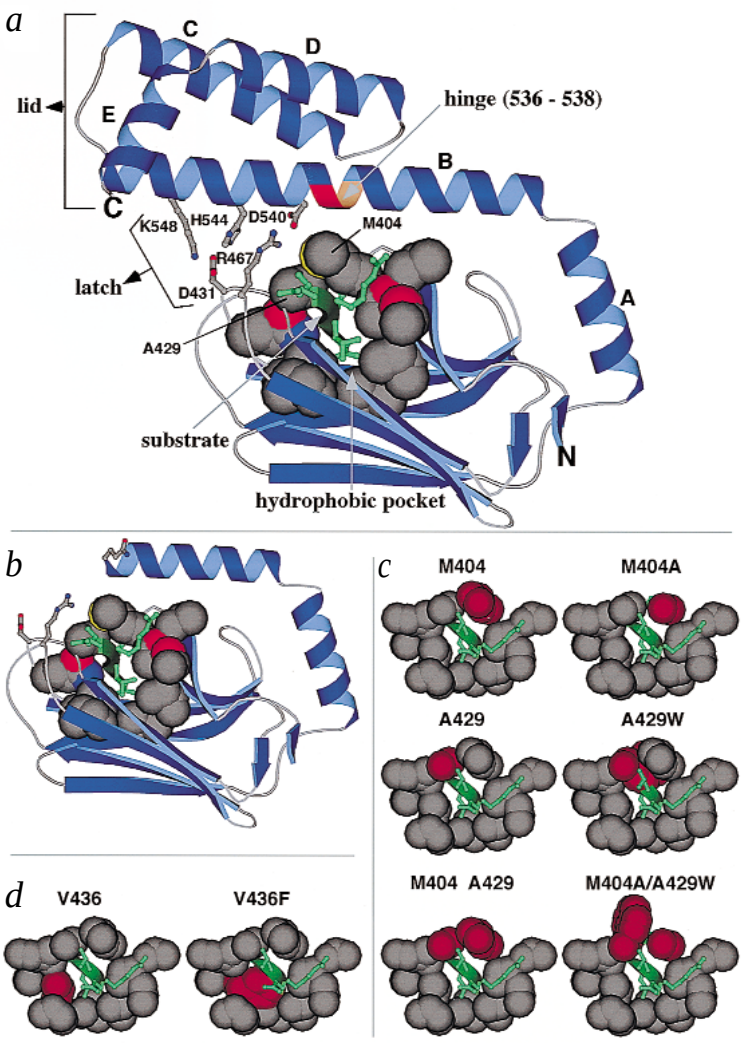

Fig. 1 Structure of DnaK wild type and mutant proteins. ***a***, Crystal structure of the wild type DnaK substrate binding domain. The amino acids that interact with the substrate peptide (green) are shown in space filling representation colored according to the nature of the atom (C, gray; N, blue; O, red; S, yellow). The latch[7] formed by a salt bridge and hydrogen bonds between amino acids of the distal part of helix B (540, 544, 548) and the outer loops (431, 467) are shown in ball and stick representation. The hinge region (amino acids 536–538) is indicated in red. ***b***, Model of the substrate binding domain of DnaK(2–538) in the same representation as for wild type DnaK in (*a*). The last amino acid, Gln 538 is shown in ball and stick representation. ***c***,***d***, Close up views of the SBC of wild type DnaK and models of (*c*) the arch and (*d*) the hydrophobic pocket mutants calculated using WhatIf[12]. Each pair of SBC views shows wild type DnaK on the left and mutant DnaK on the right. The substrate interacting amino acids are shown in space filling representation (all atoms in gray); the mutated amino acids are shown in red. Drawings made with Molscript[33].

[1]Institut für Biochemie und Molekularbiologie, Universität Freiburg, Hermann-Herder-Str.7, 79104 D-Freiburg, Germany. [2]Present address: Central Research Facility, A30, BASF AG, D-67056 Ludwigshafen, Germany.

Correspondence should be addressed to B.B. *email: bukau@sun2.ruf.uni-freiburg.de*

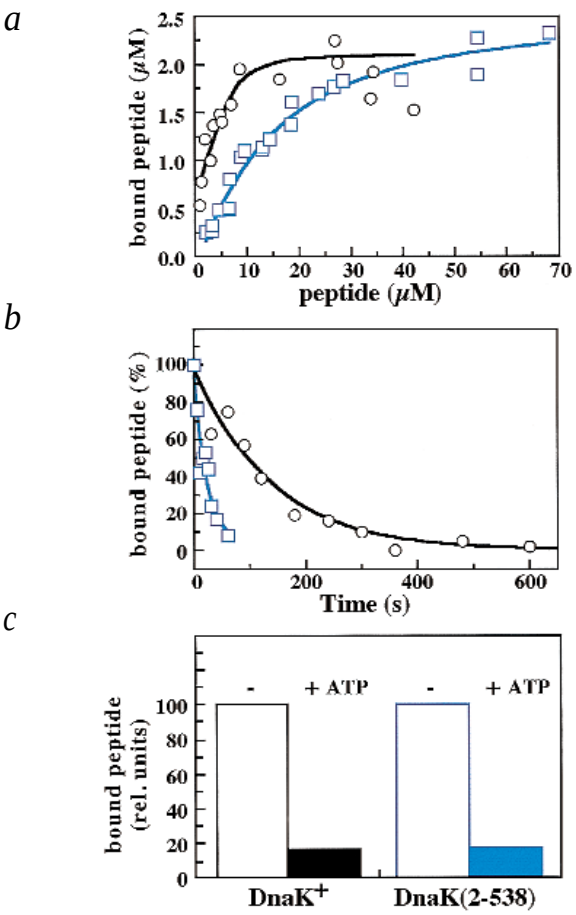

Fig. 2 Characterization of the DnaK(2–538) mutant protein. ***a***, Determination of the K_d using ^{3}H-peptide C and 7.5 μM DnaK. ***b***, Determination of k_{off} for wild type DnaK and DnaK(2–538). Black circles, DnaK$^+$; cyan squares, DnaK(2–538). ***c***, Determination of the amount of bound ^{3}H-peptide C in the absence and presence of ATP.

mined by X-ray crystallography[7]. It consists of a β-subdomain (amino acids 393–501) and a C-terminal α-helical subdomain (amino acids 509–607) (Fig. 1*a*). The peptide substrate is bound in a cavity formed by two pairs of inner and outer loops protruding upwards from the β-sandwich. The structure suggests that two elements are crucial for peptide binding: a hydrophobic pocket that accommodates a single hydrophobic side chain and an arch formed by residues Met 404 and Ala 429 that encloses the peptide backbone (Fig. 1*a*). In addition, based on distinct conformations observed in two different crystal lattices[7], it was proposed that residues 536–538 constitute a hinge for a helical lid that is closed in the ADP state but is open in the ATP state.

The crystal structure and three NMR structures[8–10] of the substrate binding domain provide revealing snapshots of Hsp70–substrate interactions, but also raise further questions about the mechanisms of these dynamic interactions. First, the proposed mechanism of the ATP-controlled opening of the SBC requires experimental verification. Second, the contributions of the key structural elements of the SBC — the hydrophobic pocket, the arch and the helical lid — to substrate binding are unclear. Third, it is uncertain whether the chaperone activity of Hsp70 requires that association with substrates occurs with high affinity. Based on *in vitro* studies of Kar2 (BiP), an Hsp 70 homolog from *Saccharomyces cerevisiae* endoplasmatic reticulum[6,11], it has been proposed that the SBC exhibits virtually no substrate specificity. Instead, Kar2 acts as a trap for almost any peptide sequence upon ATPase stimulation by the DnaJ homolog, Sec63. This proposal has been generalized to apply to other Hsp70 family members[11]. It implies that mutations in the SBC that affect substrate binding affinity would not strongly interfere with the chaperone activity of Hsp70. We have addressed these questions by dissecting the functional consequences of mutations in the substrate binding domain of DnaK.

Design of DnaK mutant proteins

To investigate the mechanism of nucleotide-controlled opening and closing of the SBC, we took advantage of a DnaK mutant protein isolated in a genetic screen for partial loss of function in *dnaK*. The *dnaK163* mutant allele carries an amber stop codon that leads to production of a DnaK mutant protein lacking the C-terminal 100 residues (DnaK(2–538)) starting exactly at the proposed hinge point for the ATP-induced movement of the lid (Fig. 1*b*). According to the proposed mechanism[7] the DnaK(2–538) mutant protein should be in a constitutively open conformation.

The role of the arch was assessed by mutating Met 404 and Ala 429, two residues forming the arch above the SBC[7]. The DnaK-M404A mutation is expected to produce a gap in the arch thus allowing substrate release, whereas the DnaK-A429W mutation is expected to generate steric hindrance hampering arch formation as well as substrate binding and release. The double mutant DnaK-M404A/A429W was used to test whether both alterations produce an additive effect or compensate for each other, because in the double mutant the positions of the large and the small hydrophobic residue are reversed when compared to the wild type protein (Fig. 1*c*). Lastly, the lid-truncated mutant was combined with the M404A alteration (DnaK(2–538)-M404A) to test whether the arch and lid act synergistically or independently.

The role of the hydrophobic pocket in substrate binding was investigated by the DnaK-V436F (Fig. 1*d*) mutant. The replacement of the highly conserved Val 436 by Phe is expected to fill the binding pocket and thereby block access of substrate side chains. Val 436 was chosen because its side chain is the only one in the pocket that points directly towards the bound Leu side chain of the cocrystallized peptide substrate[7].

To assess the effects of the introduced altertions on the structure of the substrate binding domain, we performed modeling (using the WhatIf program[12]), circular dichroism (CD), thermal

Table 1 Kinetic constants for the DnaK–σ^{32} interaction

	K_d (μM)	Relative to wt	k_{off} (s^{-1}) $\times 10^{-4}$	Relative to wt	$T_{1/2}$ (min)	k_{on}[1] (M^{-1} s^{-1})	Relative to wt
DnaK$^+$	1.4 ± 0.2	1.0	4.7 ± 0.8	1.0	25	336	1.0
DnaK-V436F	24.2 ± 2.0	17.3	4.4 ± 1.1	0.9	26	18	0.05
DnaK-M404A	3.0 ± 0.8	2.1	11.4 ± 0.9	2.4	10	380	1.1
DnaK-A429W	5.5 ± 1.4	3.9	5.2 ± 0.9	1.1	22	95	0.3
DnaK-M404A/A429W	4.3 ± 1.0	3.1	6.2 ± 1.0	1.3	19	144	0.4
DnaK(2–538)	6.7 ± 1.7	4.8	39.8 ± 5.0	8.5	3	594	1.7
DnaK(2–538)-M404A	9.3 ± 1.3	6.6	56.2 ± 7.4	12.0	2	604	1.8

[1]k_{on} values were calculated from the K_d and k_{off} values.

Table 2 Kinetic constants for the interaction of DnaK with peptide substrates

Peptides/DnaK proteins	DnaK–ADP						DnaK–ATP					
	K_d		k_{off}		k_{on}[1]		K_d		k_{off}		k_{on}[1]	
	μM	Relative to wt	s^{-1} $\times 10^{-4}$	Relative to wt	$M^{-1}\,s^{-1}$ $\times 10^{-4}$	Relative to wt	μM	Relative to wt	s^{-1}	Relative to wt	$M^{-1}\,s^{-1}$ $\times 10^{6}$	Relative to wt
σ^{32}-Q132–Q144-C-IAANS												
DnaK$^+$	0.078 ± 0.007	1.0	9.1 ± 0.2	1.0	1.17	1.0	1.8 ± 0.3	1.0	2.31 ± 0.03	1.0	1.28	1.0
DnaK-M404A	0.22 ± 0.026	2.8	32.0 ± 0.5	3.5	1.45	1.2	10.7 ± 3.6	5.9	3.73 ± 0.03	1.6	0.35	0.27
DnaK-A429W	0.32 ± 0.032	4.1	29.8 ± 0.5	3.3	0.93	0.8	6.3 ± 1.6	3.5	1.42 ± 0.01	0.6	0.23	0.18
DnaK-M404A/A429W	0.53 ± 0.071	6.8	147 ± 2	16.2	2.77	2.4	9.6 ± 3.0	5.3	3.34 ± 0.02	1.4	0.35	0.27
DnaK-V436F	3.0 ± 0.29	38.5	9.2 ± 0.2	1.0	0.03	0.03	ND		2.51 ± 0.02	1.1	ND	
^{3}H-peptide C												
DnaK$^+$	1.5	1.0	110	1.0	0.7	1.0	ND[2]		ND		ND	
DnaK(2–538)	11	7.3	600	5.4	0.5	0.7	ND		ND		ND	

[1]k_{on} values were calculated from K_d and k_{off} values.
[2]Due to the fast substrate exchange in the ATP state K_d and k_{off} values could not be determined using ^{3}H-peptide C. ND, not determined.

unfolding and partial tryptic digestion experiments. The results (not shown) indicate that no major perturbation in the local structure of the SBC occurs in the mutants.

Interactions of mutant proteins with substrates

For the wild type protein and all three classes of DnaK mutants we investigated substrate interactions in the ADP state using a native protein substrate, the *E. coli* heat shock transcription factor σ^{32}, and in the ADP and ATP state using a peptide derived from σ^{32} labeled with the fluorophore IAANS (σ^{32}-Q132–Q144-C-IAANS)[13]. For the DnaK(2–538) mutant protein a radiolabeled peptide (^{3}H-peptide C; ref 14) was used because this mutant protein failed to give signals with fluorescently labeled peptides (data not shown).

The dissociation equilibrium (K_d) constants for the hydrophobic pocket variant DnaK-V436F in the ADP state in complex with σ^{32} and σ^{32}-Q132–Q144-C-IAANS were 17- and 38-fold larger than that of the wild type DnaK, respectively (Fig. 3; Tables 1, 2). In the ATP state, the mutant protein had such a low affinity for σ^{32}-Q132-Q144-C-IAANS that fluorescence measurements were not possible. These large increases in K_d in the ADP and ATP states resulted solely from a dramatic decrease in k_{on} since the k_{off} values were identical to those of the wild type (Tables 1, 2). These results demonstrate the large contribution of the hydrophobic pocket to substrate affinity and the importance of the interaction of DnaK with the side chain of a single residue in the substrate.

The K_d values for DnaK(2–538) in the ADP state in complex with σ^{32} and ^{3}H-peptide C were 5- and 7-fold larger than those of wild type DnaK, respectively (Table 1; Fig. 2*a*). These increases in K_d for DnaK(2–538) resulted mainly from a 5- to 8.5-fold accelerated k_{off} (Table 1; Fig. 2*b*), while the calculated k_{on} for DnaK(2–538) was almost identical to that of wild type DnaK (Tables 1, 2). ATP strongly increased substrate release for DnaK(2–538) and wild type DnaK (Fig. 2*c*), indicating that ATP leads to a further decrease in affinity for substrates.

The K_d values for the three arch mutants in the ADP state in complex with peptide σ^{32}-Q132–Q144-C-IAANS and peptide substrates were 2- to 7-fold larger than that of the wild type, indicating that the arch makes a significant contribution to substrate affinity. The arch mutants interacted with σ^{32} in the manner as predicted (Table 1) — that is, opening of the arch (DnaK-M404A) increased the k_{off} with little effect on the k_{on}, while indroducing steric hindrance (DnaK-A429W) mainly

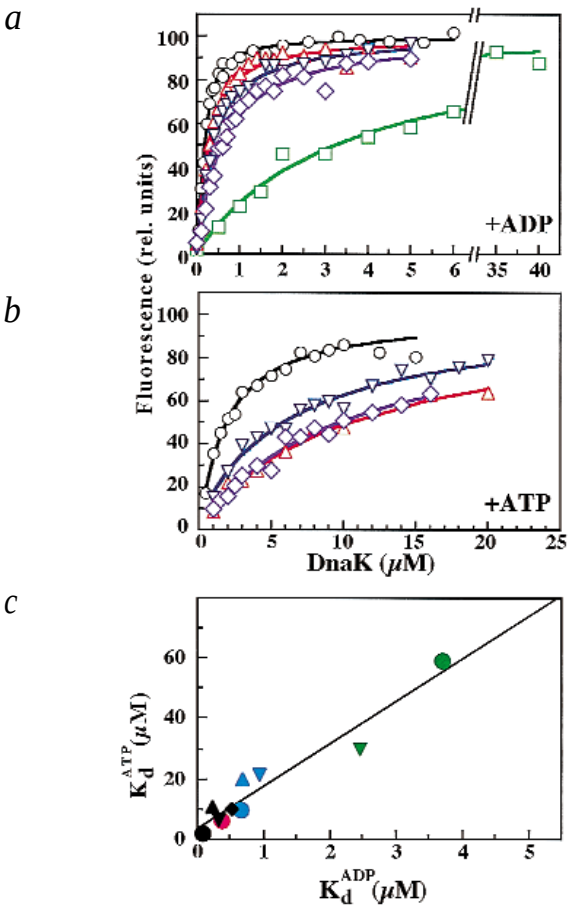

Fig. 3 Peptide binding to wild type and mutant DnaK. The K_d values of wild type and mutant DnaK proteins were determined using a fluorescently labeled peptide σ^{32}-Q132–Q144-C-IAANS. ***a***, DnaK in the ADP state. ***b***, DnaK in the ATP state. Black circles, DnaK$^+$; red triangles, DnaK-M404A; blue inverted triangles, DnaK-A429W; purple diamonds, DnaK-M404A/A429W; green squares, DnaK-V436F. ***c***, Comparison of the dissociation constants of wild type and mutant DnaK–ADP and DnaK–ATP for a series of different peptides; σ^{32}-Q132–Q144-C (QRKLFFNLRKTKQC; black), σ^{32}-M195–N207-C (MAPVLYLQDKSSNC; magenta), σ^{32}-E115–A127-C(L118A) (EYVARNWRIVKVAC; cyan), a-p1 (CALLQSR; green). Circles, DnaK$^+$; triangles, DnaK-M404A; inverted triangles, DnaK-A429W; diamonds, DnaK-M404A/A429W. Linear regression analysis of the K_d values gave a correlation coefficient of 0.9618.

decreased the k_{on}. Unexpectedly, however, the k_{off} for the complex of DnaK-A429W with σ^{32} was slightly increased instead of decreased. This may indicate that the Trp residue weakens the closed conformation as defined by a closed arch and a closed lid (Fig. 1*a*), possibly by interfering sterically with the interactions between the helical lid and the outer loops (latch; as described in Fig. 1*a*). The double DnaK-M404A/A429W mutant showed intermediary effects on both k_{on} and k_{off}, suggesting that the effects of the two mutations compensate for each other. For all the complexes of the arch mutants with the σ^{32}-Q132–Q144-C-IAANS peptide, the decrease in K_d was mainly caused by an increased k_{off}. This also supports the idea that the Trp residue in DnaK-A429W and DnaK-M404A/A429W interferes sterically with the closing mechanism, — that is, the arch formation and the interaction of the lid with the outer loops. The role of steric hindrance in substrate binding does not seem to be as important for the peptide as for σ^{32}, probably because of the higher diffusional mobility and flexibility of the peptides (Fig. 3; Table 2).

In the ATP state, the K_d of the DnaK–σ^{32}-Q132–Q144-C-IAANS complex was increased 3.5- to 6-fold for the arch mutants compared to wild type (Table 2); this resulted from a 4- to 5-fold decrease in k_{on}. The finding that k_{on} decreased even for DnaK-M404A is consistent with Met 404 having a role in making initial substrate contacts.

To test whether the arch and lid act synergistically, we measured the K_d and k_{off} of the lid truncated arch mutant DnaK(2–538)-M404A binding to σ^{32} in the ADP state. The K_d and k_{off} values increased 6.6- and 12-fold, respectively, compared to wild type. This indicates that the effects of this mutant on K_d and k_{off} are additive rather than synergistic. The binding parameters of this mutant protein to fluorescently or radioactively labeled peptide were not determined because of a lack of fluorescent signal and very fast k_{off} rates. In summary, these data indicate that the lid and the arch both influence the kinetics of substrate binding and release. Furthermore, they affect substrate binding in an additive manner.

Correlation of K_d values in ADP and ATP states

A comparison of the K_d values for wild type DnaK–ADP and DnaK–ATP binding to σ^{32}-Q132-Q144-C-IAANS revealed that ATP increases the K_d by 20-fold, which is consistent with other studies[2,15–17]. The increase in K_d values for all tested DnaK mutants in the ADP state was smaller than that of wild type (~2- to 7-fold; Tables 1, 2). Thus, additional conformational changes in the β-sandwich domain are necessary for the ATP-driven opening of the SBC.

To dissect the effects of ATP further, we investigated whether the residues of DnaK contacting the substrate in the ATP state change upon ATP hydrolysis. Because ATP binding must induce opening of the lid, the arch, and the loops and β-strands forming the SBC, the relative affinities of DnaK in the ATP and ADP states are likely to differ for different substrates if the residues contacting the substrates change depending on the states of the bound nucleotide. For example, in the DnaK–peptide crystal structure (which is presumably in the ADP state), the arch residue Met 404 contacts a Leu side chain of the peptide substrate and thereby contributes to DnaK's preference for large aliphatic residues[18] in the ADP state. It is possible, however, that Met 404 does not make such a contribution in the open ATP state of DnaK; therefore, the presence or absence of a Leu residue at this position would not affect binding affinity in the ATP state. To test these possibilities we determined the K_d values for the binding of four peptides with unrelated sequences to wild type DnaK in the ADP and ATP states. An excellent correlation (r = 0.9998) existed between the K_d values of each peptide binding to wild type DnaK–ADP and DnaK–ATP (Fig. 3*c*, circles). We also determined the K_d values of DnaK-M404A and DnaK-A429W in the ADP and ATP states binding to those peptides for which the K_d values are in the experimentally accessible range. The K_d values of each of the different peptides in complex with the mutants in the ADP and ATP states also correlated with each other, although slightly less stringently compared to wild type (Fig. 3*c*). It is possible that the regression line for each individual mutant is shifted or tilted slightly compared to wild type and to other DnaK mutants. This could explain why K_d values for binding of certain peptides with different DnaK mutants in the ADP and ATP states are not tightly correlated (Table 2). However, the overall correlation of all presented data points for wild type and mutant proteins and different peptides is high (r = 0.9618). This finding is consistent with the idea that substrates, at least initially, interact with the same residues of DnaK, and in a similar way, in the ADP and ATP states.

ATPase stimulation correlates with affinity

The key step of the functional cycle of DnaK, the locking-in of substrates by ATP hydrolysis, is mediated by the concerted action

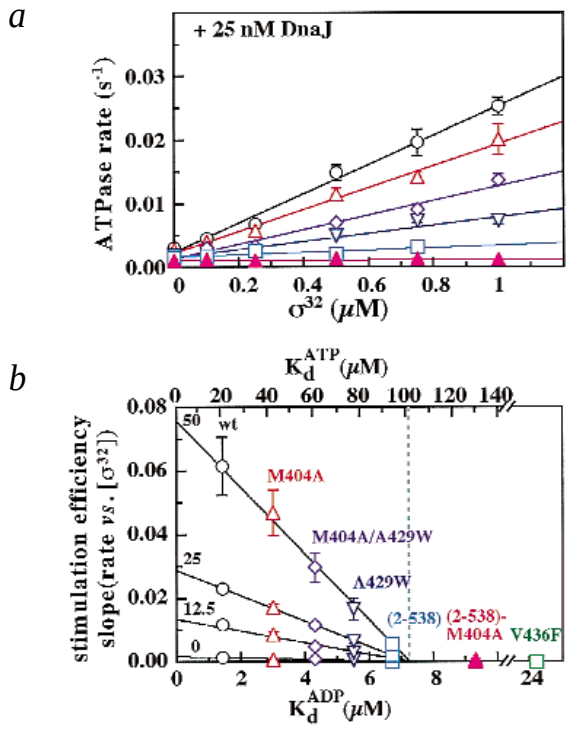

Fig. 4 ATPase stimulation correlates with substrate affinity. ***a***, Dependence of the ATPase rate of wild type and mutant DnaK on the concentration of σ^{32} in the presence of 25 nM DnaJ. ***b***, Plot of the slope of the lines shown in (*a*) and similar lines determined in the absence and in the presence of DnaJ (12.5 and 50 nM) *versus* the K_d of wild type and mutant DnaK–ADP for σ^{32} (correlation coefficients: 0 nM DnaJ, 0,9719; 12.5 nM DnaJ, 0.9715; 25 nM DnaJ, 0.9994; 50 nM DnaJ, 0.9979). The second abscissa on top indicates the K_d values in the ATP state calculated from the regression line in Fig. 3*c*. The dashed line indicates the threshold of 7.3 μM (DnaK–ADP) and 100μM (DnaK–ATP) (see text for explanation). Black circles, DnaK$^+$; red triangles, DnaK-M404A; blue inverted triangles, DnaK-A429W; purple diamonds, DnaK-M404A/A429W; cyan squares, DnaK(2–538); pink triangles, DnaK(2–538)-M404A; green squares, DnaK-V436F.

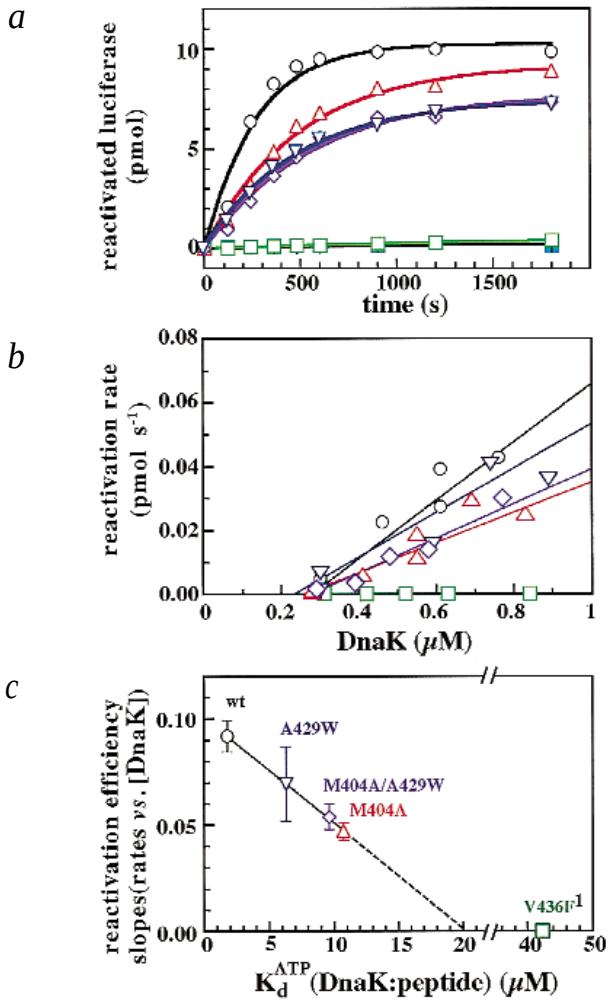

Fig. 5 Refolding of chemically denatured luciferase. ***a***, Kinetic of the reactivation of GdnHCl-denatured luciferase by 0.55 μM wild type or mutant DnaK, DnaJ and GrpE as described in the Methods. The solid lines are the single exponential fits to the experimental data. ***b***, Graph of the initial reactivation rate *versus* the DnaK concentration. Correlation coefficients: 0.987 for wild type DnaK, 0.981 for DnaK-M404A, 0.892 for DnaK-A429W and 0.976 for DnaK-M404A/A429W. ***c***, Plot of the slopes in (*b*) *versus* the K_d of DnaK–ATP for the peptide σ^{32}-Q132–Q144-C-IAANS. The K_d value for DnaK-V436F was calculated according to the regression line in Fig. 3*c*. Black circles, DnaK$^+$; red triangles, DnaK-M404A; blue inverted triangles, DnaK-A429W; purple diamonds, DnaK-M404A/A429W; green squares, DnaK-V436F; cyan squares, DnaK(2–538); +, no DnaK (not readily visible because overlayed by the square symbols).

of DnaJ and protein substrates[4,5]. To investigate whether this step is sensitive to changes in substrate affinity and substrate binding kinetics we analyzed the ability of σ^{32} and DnaJ to stimulate ATP hydrolysis of the DnaK mutant proteins. ATP hydrolysis rates were determined in single turnover experiments after addition of increasing concentrations of σ^{32} with or without limiting concentrations of DnaJ (12.5, 25 and 50 nM). The ATPase rates increased linearly with increasing σ^{32} concentration (Fig. 4*a*), and the slope is a measure of the efficiency with which σ^{32} stimulates ATP hydrolysis by DnaK (stimulation efficiency). The DnaK mutant proteins that had a lower affinity for σ^{32} were stimulated less efficiently. Moreover, the stimulation efficiency tightly correlated with the K_d values of complexes between σ^{32} and the DnaK proteins in the ADP state (Fig. 4*b*). For the DnaK(2–538)-M404A and DnaK-V436F mutant proteins, which have K_d values of 9.3 and 24 μM for σ^{32}, no stimulation of the DnaK ATPase activity was observed, indicating that the DnaJ and substrate-dependent locking-in mechanism requires a threshold affinity. It is important to emphasize that under the single turnover conditions (as in Fig. 4*a*), when preformed DnaK–ATP complexes were assayed, the only interaction relevant for stimulation of ATP hydrolysis is between σ^{32} and DnaK–ATP. The efficiency of ATPase stimulation correlated with the K_d of DnaK in the ADP state for σ^{32} (Fig. 4*b*). This indicates that the affinities of DnaK in the ADP and the ATP states for protein substrates correlate with each other as demonstrated in Fig. 3*c* for peptide substrates.

Chaperone activity depends on substrate affinity

It has been proposed that the assisted folding activity of Hsp70 is largely independent of the affinity of Hsp70 for substrates[6,11]. The described DnaK mutants with their defined alterations in substrate affinity allow this proposal to be experimentally tested.

Chemically denatured luciferase was diluted into refolding buffer containing DnaK, DnaJ, GrpE and ATP. The DnaK(2–538) and DnaK-V436F mutants completely lacked refolding activity while the arch mutant proteins were partially active (Fig. 5*a*). The refolding rates at DnaK concentrations between 0.3–1 μM were determined by fitting the experimental data to first order kinetics. These rates increased linearly with the concentration of DnaK (Fig. 5*b*). The slopes of these lines represent the efficiency of luciferase refolding by the DnaK variants. We compared the efficiency of luciferase refolding with the affinities of the DnaK mutants for peptide substrate. Both substrates are likely to be in an extended conformation, at least at the segment that associates with DnaK, and are therefore suitable for this comparison. The plot of the refolding efficiencies (slopes in Fig. 5*b*) *versus* the affinity (K_d) of DnaK–ATP for the peptide substrate σ^{32}-Q132-Q144-C-IAANS is shown in Fig. 5*c*. The clear correlation demonstrates that the efficiency of luciferase refolding is strongly influenced by the affinity of DnaK-ATP for substrates.

In vivo consequences of the DnaK alterations

We investigated the consequences of the mutations in the SBC for the *in vivo* activities of DnaK. Two essential activities were tested, the assistance of protein folding during heat stress conditions and the replication of bacteriophage λ DNA. We expressed wild type and mutant *dnaK* alleles from plasmids under IPTG control in two strains deficient in DnaK function, BB1553 (ref. 19) and CG800 (ref. 20); these carry the *ΔdnaK52* and *dnaK103*(*am*) mutations, respectively. Both strains are completely devoid of a functional DnaK protein. The main difference between the two strains is the concentration of the cochaperone DnaJ which is, at the most, 5% of the wild type level in BB1553 (A. Mogk, pers. comm.) and ~200% of the wild type level in CG800. The non-permissive temperature range starts at 37 °C for BB1553 and 41 °C for CG800. Similar results were obtained with both strains (summarized in Table 3 for BB1553). Only the *dnaK-M404A* allele complemented the temperature sensitive phenotypes of the *ΔdnaK52* allele with the same efficiency as wild type *dnaK*. The *dnaK-V436F* allele completely failed to complement the phenotype, the *dnaK-A429W* allele did so only marginally in the presence of 250 μM IPTG, while the *dnaK-M404A/A429W* allele did so more efficiently but not completely. These complementation efficiencies correlate well with the efficiencies by which DnaJ and substrate stimulate ATP hydrolysis by these mutant proteins *in vitro*. The *dnaK163* allele (encoding DnaK(2–538)) and the mutant allele encoding DnaK(2–538)-M404A (data not shown)

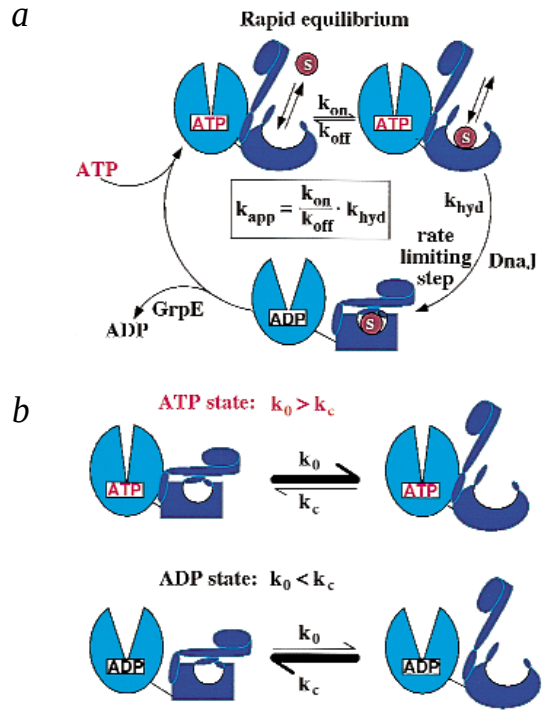

Fig. 6 Model of the interaction of the Hsp70 chaperones with substrates. ***a***, Initial interaction of the substrate with DnaK in the open conformation determines the efficiency with which DnaK traps the substrate and therefore the speed of the chaperone cycle. ***b***, ATP and ADP state may only differ in the frequency of transition between an open and closed conformation. k_o, opening rate; k_c, closing rate.

complemented the temperature sensitive phenotype of the *ΔdnaK52* allele only at high IPTG concentrations (500 μM). Qualitatively similar results were obtained for the lytic growth of bacteriophage λ (Table 3). Overall, these results correlate well with the *in vitro* defects of the DnaK mutant proteins. These results support our *in vitro* analysis and further highlight the importance of high affinity substrate binding for the chaperone activity of DnaK.

Our analysis has generated three major conclusions important for understanding the mechanism of the Hsp70 chaperone activity. The first conclusion concerns the coupling mechanism that allows ATP to control substrate release. Deletion of the α-helical subdomain, starting at the proposed hinge point at residue 538, increased k_{off} for DnaK–substrate complexes, and thus this region constitutes a physical lid-like barrier to substrate release as has been proposed[7]. However, the truncated mutant protein was not in the constitutively open conformation since k_{off} in the ADP state was only 5-fold higher than that of wild type DnaK. By contrast, k_{off} of wild type DnaK increases ~2,500-fold in the presence of ATP (Table 2). Furthermore, the truncated DnaK partially complement the temperature sensitive phenotype of a *ΔdnaK* strain and allows λ plaque formation in a *dnaK* deficient host. Our data are consistent with a recent NMR study using a truncated DnaK (residues 1–507; ref. 10) and two biochemical studies showing that a similar truncation of mammalian cytosolic Hsc70 (Hsc70(1–540)) still allows chaperone-dependent uncoating of clathrin coated vesicles[21] and that truncated Kar2 shows reduced peptide binding upon addition of ATP (ref. 6). The coupling mechanism that allows ATP binding to accelerate substrate release thus must operate through the 150 residues adjacent to the ATPase domain and not primarily through the lid.

The second conclusion is the establishment of a relationship between the substrate affinity, chaperone activity and ATPase activity of DnaK. The K_d values of DnaK–ATP interactions with substrates were tightly correlated with those of DnaK–ADP (Fig. 3*c*). We therefore propose that the conformation of DnaK that leads to association with substrates (the open conformation) is highly similar in the ADP and ATP states, and that the differences in k_{on} and k_{off} between these states are a consequence of the different probabilities of opening the lid, arch and loops as well as the β-sheets forming the SBC including the hydrophobic pocket (see below and Fig. 6*b*). The K_d of a DnaK–substrate complex in the ADP state is therefore a meaningful value, despite the fact that during its functional cycle DnaK interacts with the substrate in the ATP state and then hydrolyzes ATP to lock in the substrate.

Our analysis revealed that the substrate-mediated stimulation of the ATPase rate tightly correlated with the affinity of DnaK for the substrate. Extrapolation of the data suggests that DnaK mutant proteins with a K_d value for a given substrate that is higher than ~7 μM in the ADP state (100 μM for DnaK–ATP) cannot be stimulated by that substrate (indicated by the dashed line in Fig. 4*b*). This suggestion was verified by two mutant proteins, DnaK(2–538)-M404A and DnaK-V436F, which have K_d values with σ^{32} of 9.3 μM and 24 μM, respectively, and could not be stimulated by this substrate and DnaJ. In contrast, DnaK(2–538), which had a K_d of 6.7 μM, was stimulated, although only very weakly (Fig. 4*a*,*b*). Based on our results with σ^{32} and DnaK mutant proteins we deduce that substrates with K_d values for wild type DnaK–ADP higher than 7 μM should not be able to stimulate ATP hydrolysis of wild type DnaK.

Our findings also have implications for the recently proposed two-signal mechanism for stimulation of ATP hydrolysis[4–6]. DnaJ was proposed to interact with substrates first and subsequently transfer them to DnaK–ATP. Simultaneous interaction of DnaK with DnaJ and the substrate triggers ATP hydrolysis and locking-in of substrates[5,22,23]. This mechanism would not only allow DnaJ to pre-select the DnaK substrates but could possibly circumvent the limitation of DnaK's affinity for substrates. Our data show that DnaK's affinity for substrates determines the efficiency with which ATP hydrolysis is stimulated even in the presence of DnaJ. Furthermore, the efficiency of DnaK-assisted

Table 3 Complementation of the Δ*dnaK*52 phenotype

	Temperature sensitivity[1] IPTG (μM)					λ sensitivity[2] IPTG (μM)		
ΔdnaK52	0	50	100	250	500	0	100	250
-	-	-	-	-	-	-	-	-
dnaK$^+$	-	-	0.11	0.85	0.006	-	1	1
dnaK163	-	-	-	0.0001	0.3	-	-	0.1
dnaK-M404A	-	-	0.15	1	0.05	-	1	1
dnaK-A429W	-	-	-	0.35	0.001	-	0.05	0.6
dnaK-M404A/A429W	-	-	-	0.95	0.03	-	1	0.2
dnaK-V436F	-	-	-	-	-	-	-	-

[1]Dilutions of these cultures were spotted onto LB plates containing ampicillin, kanamycin, and the indicated concentrations of IPTG. The number of colonies after 18 h at 40 °C relative to the number of colonies of the strain expressing wild type *dnaK* at 30 °C are shown. [2]To test the ability of the mutant *dnaK* allels to support λ plaque formation (λ sensitivity), dilutions of a λ_{vir} lysate were spotted onto top agar containing cells of the indicated strain and IPTG concentration. The number of plaques relative to the plaque number on the strain expressing wild type *dnaK* in the presence of 100 μM IPTG is shown.

refolding of a denatured protein, firefly luciferase, correlated with its affinity for substrates, indicating that the affinity of DnaK for substrates is crucially important for the DnaJ-mediated initiation of the functional cycle (Fig. 6*a*).

This scenario is different from a recently proposed mechanism for Sec63-mediated interaction of Kar2 (BiP) with translocating polypeptide chains suggesting that Kar2 serves as a nonspecific trap that closes with the binding of any peptide sequence provided that ATP is present and Sec63 is in close proximity[6,11]. Our study provides evidence that such a nonspecific trap mechanism is not applicable for DnaK. Whether BiP differs from DnaK with respect to this basic mechanism of substrate recognition is unclear, although the very similar sequences of the protein domains involved suggest similarity in functional mechanism. It may be, however, that the K_d cut-off for stimulation of ATP hydrolysis by a substrate differs between DnaK and Kar2.

The third conclusion of our study is the assignment of roles for the individual structural components of the SBC in substrate interaction. Blocking the access to the central hydrophobic pocket caused the largest decrease in affinity for substrates. Interestingly, the hydrophobic pocket mutant protein (DnaK-V436F) released peptide and protein substrates with the same rate constant as wild type DnaK, in both the ADP and the ATP states. The substrate may thus be bound in the same way as in the wild type protein despite the steric crowding in the hydrophobic pocket.

Mutations in the arch decreased the affinity of DnaK–ADP for substrates by 3- to 7-fold, largely due to increased k_{off}. Substrate release was affected despite the presence of the stabilizing latch residues forming the salt bridge and hydrogen bonds between helix B and the outer loops. This indicates that the arch has a distinct role in controlling the k_{off} of substrates. Interestingly, the arch-forming residues are the only substrate-interacting amino acids that have been subject to considerable evolutionary variations within the Hsp70 family, possibly reflecting functional differences between homologs[24].

Our data suggest a highly dynamic mechanism operating on the DnaK substrate binding domain (Fig. 6*b*). In both the ADP and the ATP state, the SBC opens and closes periodically. The main differences between the two states are the rates for opening (k_o) and closing (k_c) — in the ATP state $k_o > k_c$ and in the ADP state $k_o < k_c$. This dynamic mechanism is further supported by two findings. First, substrates can associate at significant rates with DnaK–ADP ($T_{1/2}$ = 1–100 min at 1 μM DnaK and 1 μM substrate). Since a lateral sliding of substrates into the closed SBC is ruled out by structural data[7], the SBC has to open up occasionally even in the ADP state to allow substrate association. Second, the association rates of peptides to DnaK–ATP (~10^6 M^{-1} s^{-1}; ref. 2 and this study) are far from being diffusion controlled (~10^9 M^{-1} s^{-1}), in contrast with the association of peptide with the SecB chaperone[25,26]. In view of our model, this finding can be explained by assuming that even in the ATP state the SBC is occasionally in the closed conformation, which would render a collision interaction between DnaK and a substrate unproductive.

In conclusion, our results indicate that DnaK–substrate interactions rely on: (i) a central pocket that is a major contributor to the substrate binding energy, (ii) a two-gated closing device in the SBC involving an arch and a helical lid, and (iii) an ATP-controlled mechanism that operates through a largely β-structured subdomain. This multistep mechanism controls the affinity of DnaK for substrates, which in turn is the central determinant of the chaperone activity of DnaK.

Methods

Bacteria and phages. *In vivo* experiments were performed in strains BB1553 (MC4100 *ΔdnaK52 sidB1*; ref. 19) and CG800 (C600 *dnaK103 thr*:Tn*10*; ref. 20). λ plaque formation was tested using λ_{vir} and, as control, a *dnaK* and *dnaJ* transducing λ phage (a gift from C. Georgopoulos).

Mutant construction and protein purification. *dnaK* mutant alleles were constructed according to ref. 27. For purification, DnaK mutant proteins and GrpE were produced in a *ΔdnaK52* background and purified as described[28]. The DnaJ purification protocol will be published elsewhere (H.J. Schönfeld, pers. comm.). DnaK mutant proteins were verified by electrospray mass spectrometry.

Determination of the dissociation constants. The dissociation equilibrium constants of DnaK mutant proteins in the ADP state with σ^{32} were determined as described[29]. ^{3}H-σ^{32} (1 μM) was incubated with different concentrations of DnaK (5–50 μM) in a total volume of 20 μl at 30 °C for at least 2 h. Bound and free ^{3}H-σ^{32} were separated by gel filtration on a superdex 200 column (10/30HR, Pharmacia) at 4 °C and the amounts determined by scintillation counting. The K_d was calculated from the Scatchard plot analysis of the data. Peptide binding to DnaK was studied using a 2-(4′-(iodoacetamido)anilino)naphthalene-6-sulfonic acid (IAANS)-labeled peptide (0.1 μM for wild type and arch mutant proteins and 0.5 μM for DnaK-V436F) according to ref. 13. To determine peptide binding to DnaK-ATP, σ^{32}-Q132–Q144-C-IAANS (0.2 μM) was incubated with DnaK–ADP (0.5 to 20 μM) for 1 h. ATP was added to a final concentration of 1 mM and the decrease in fluorescence emission at 460 nm (excitation at 335 nm) was recorded for 200 s, after which time the equilibrium between bound and free peptide was reached. Peptide binding to DnaK–ADP was determined similarly except that no ATP was added. The fluorescence values were plotted against the DnaK concentration and the data fit to the quadratic solution using the Grafit program version 3.0 (Erithacus Software).

The dissociation rate constants for peptides were determined by preincubating 0.5 μM σ^{32}-Q132–Q144-C-IAANS with 0.5 μM DnaK (for DnaK-V436F 5 μM peptide and 5 μM protein) for 1 h. After addition of 50 μM unlabeled σ^{32}-Q132-Q144 and rapid mixing fluorescence was recorded. Peptide release in the presence of ATP was monitored in a stopped-flow device (Applied Photophysics) using nucleotide-free DnaK prepared as described[30]. The nucleotide free status of DnaK was verified by reverse phase HPLC under denaturing conditions. Binding and release of ^{3}H-peptide C was determined as described[31].

ATPase and chaperone assays. ATPase rates of DnaK wild type and mutant proteins were performed under single turnover conditions as described[29,31]. Refolding of denatured luciferase was performed as published[32].

Acknowledgments

We thank B. Krauβ for technical assistance and W. Haehnel and R. Loyal for peptide synthesis. This work was supported by grants from the DFG and the Fonds der Chemie to B.B.

Received 21 March, 2000; accepted 25 May, 2000.

1. Buchberger, A. *et al.* Nucleotide-induced conformational changes in the ATPase and substrate binding domains of the DnaK chaperone provide evidence for interdomain communication. *J. Biol. Chem.* **270**, 16903–16910 (1995).
2. Schmid, D., Baici, A., Gehring, H. & Christen, P. Kinetics of molecular chaperone action. *Science* **263**, 971–973 (1994).
3. Bukau, B. & Horwich, A.L. The Hsp70 and Hsp60 chaperone machines. *Cell* **92**, 351–366 (1998).
4. Karzai, A.W. & McMacken, R. A bipartite signaling mechanism involved in DnaJ-mediated activation of the *Escherichia coli* DnaK protein. *J. Biol. Chem.* **271**, 11236–11246 (1996).
5. Laufen, T. *et al.* Mechanism of regulation of Hsp70 chaperones by DnaJ co-chaperones. *Proc. Natl. Acad. Sci. USA* **96**, 5452–5457 (1999).
6. Misselwitz, B., Staeck, O. & Rapoport, T.A. J proteins catalytically activate Hsp70 molecules to trap a wide range of peptide sequences. *Mol. Cell* **2**, 593–603 (1998).
7. Zhu, X. *et al.* Structural analysis of substrate binding by the molecular chaperone DnaK. *Science* **272**, 1606–1614 (1996).
8. Morshauser, R.C. *et al.* High-resolution solution structure of the 18 kDa substrate-binding domain of the mammalian chaperone protein Hsc70. *J. Mol. Biol.* **289**, 1387–1403 (1999).
9. Wang, H. *et al.* NMR solution structure of the 21 kDa chaperone protein DnaK substrate binding domain: a preview of chaperone–protein interaction. *Biochemistry* **37**, 7929–7940 (1998).
10. Pellecchia, M. *et al.* Structural insights into substrate binding by the molecular chaperone DnaK. *Nature Struct. Biol.* **7**, 298–303 (2000).
11. Matlack, K.E.S., Misselwitz, B., Plath, K. & Rapoport, T.A. BiP acts as a molecular ratchet during posttranslational transport of prepro-α factor across the ER membrane. *Cell* **97**, 553–564 (1999).
12. Vriend, G. A molecular modeling and drug design program. *J. Mol. Graph.* **8**, 52–56 (1990).
13. McCarty, J.S. *et al.* Regulatory region C of the *E. coli* heat shock transcription factor, σ^{32}, constitutes a DnaK binding site and is conserved among eubacteria. *J. Mol. Biol.* **256**, 829–837 (1996).
14. Flynn, G.C., Chappell, T.G. & Rothman, J.E. Peptide binding and release by proteins implicated as catalysts of protein assembly. *Science* **245**, 385–390 (1989).
15. Takeda, S. & McKay, D.B. Kinetics of peptide binding to the bovine 70 kDa heat shock cognate protein, a molecular chaperone. *Biochemistry* **35**, 4636–4644 (1996).
16. Greene, L.E., Zinner, R., Naficy, S. & Eisenberg, E. Effect of nucleotide on the binding of peptides to 70-kDa heat shock protein. *J. Biol. Chem.* **270**, 2967–2973 (1995).
17. Pierpaoli, E.V., Gisler, S.M. & Christen, P. Sequence-specific rates of interaction of target peptides with the molecular chaperones DnaK and DnaJ. *Biochemistry* **37**, 16741–16748 (1998).
18. Rüdiger, S., Germcroth, L., Schneider-Mergener, J. & Bukau, B. Substrate specificity of the DnaK chaperone determined by screening cellulose-bound peptide libraries. *EMBO J.* **16**, 1501–1507 (1997).
19. Bukau, B. & Walker, G.C. *ΔdnaK* mutants of *Escherichia coli* have defects in chromosomal segregation and plasmid maintenance at normal growth temperatures. *J. Bacteriol.* **171**, 6030–6038 (1989).
20. Spence, J., Cegielska, A. & Georgopoulos, C. Role of *Escherichia coli* heat shock proteins DnaK and HtpG (C62.5) in response to nutritional deprivation. *J. Bacteriol.* **172**, 7157–7166 (1990).
21. Ungewickell, E., Ungewickell, H. & Holstein, S.E.H. Functional interaction of the auxilin J domain with the nucleotide- and substrate-binding modules of Hsc70. *J. Biol. Chem.* **272**, 19594–19600 (1997).
22. Gamer, J. *et al.* A cycle of binding and release of the DnaK, DnaJ and GrpE chaperones regulates activity of the *E. coli* heat shock transcription factor σ^{32}. *EMBO J.* **15**, 607–617 (1996).
23. Schröder, H., Langer, T., Hartl, F.-U. & Bukau, B. DnaK, DnaJ, GrpE form a cellular chaperone machinery capable of repairing heat-induced protein damage. *EMBO J.* **12**, 4137–4144 (1993).
24. Rüdiger, S. Buchberger, A. & Bukau, B. Interaction of Hsp70 chaperones with substrates. *Nature Struct. Biol.* **4**, 342–349 (1997).
25. Stenberg, G. & Fersht, A.R. Folding of barnase in the presence of the molecular chaperone SecB. *J. Mol. Biol.* **274**, 268–275 (1997).
26. Fekkes, P., den Blaauwen, T. & Driessen, A.J.M. Diffusion-limited interaction between unfolded polypeptides and the *Escherichia coli* chaperone SecB. *Biochemistry* **34**, 10078–10085 (1995).
27. Kunkel, T.A., Bebenek, K. & McClary, J. Efficient site-directed mutagenesis using uracil-containing DNA. *Methods Enzymol.* **204**, 125–139 (1991).
28. Buchberger, A., Schröder, H., Büttner, M., Valencia, A. & Bukau, B. A conserved loop in the ATPase domain of the DnaK chaperone is essential for stable binding of GrpE. *Nature Struct. Biol.* **1**, 95–101 (1994).
29. Mayer, M.P., Laufen, T., Paal, K., McCarty, J.S. & Bukau, B. Investigation of the interaction between DnaK and DnaJ by surface plasmon resonance. *J. Mol. Biol.* **289**, 1131–1144 (1999).
30. Theyssen, H., Schuster, H.-P., Bukau, B. & Reinstein, J. The second step of ATP binding to DnaK induces peptide release. *J. Mol. Biol.* **263**, 657–670 (1996).
31. McCarty, J.S., Buchberger, A., Reinstein, J. & Bukau, B. The role of ATP in the functional cycle of the DnaK chaperone system. *J. Mol. Biol.* **249**, 126–137 (1995).
32. Szabo, A. *et al.* The ATP hydrolysis-dependent reaction cycle of the *Escherichia coli* Hsp70 system-DnaK, DnaJ and GrpE. *Proc. Natl. Acad. Sci. USA* **91**, 10345–10349 (1994).
33. Kraulis, J. MOLSCRIPT: A program to produce both detailed and schematic plots of protein structures. *J. Appl. Crystallogr.* **24**, 946–950 (1991).